Supplement

Philippos Garefalakis[1], Fritz Schlunegger[1]

[1]DInstitute of Geological Sciences, University of Bern, Bern, CH-3012, Switzerland

Correspondence to: Philippos Garefalakis (philippos.garefalais@geo.unibe.ch)

1 Reconstructions of palaeo-bathymetrical conditions

1.1 Reconstruction of the water depth from ripple-marks morphometry and grain size

The palaeo-bathymetrical conditions were derived from sedimentary structures such as symmetric- and asymmetric-ripple-marks. These bedforms need bottom oscillatory waves to form (Komar and Miller, 1973). Accordingly, the morphometry and grain side of these bedforms bear information about the velocity of the oscillatory currents, which can be used as basis to calculate palaeo-water depth conditions (Allen, 1981). In addition, the orientation of asymmetric ripple-marks and preserved ripple-crests allow to interpret the flow direction and the orientation of the coastline during their formation (Clifton and Dingler, 1984).

In the past years, several authors have used field-based data on the spacing λ, the height h and the median grain size D of oscillatory ripple-marks in various environments to estimate of palaeo-wave conditions (e.g. Tanner, 1971; Komar and Miller, 1973; Allen, 1981; Clifton and Dingler, 1984; Diem, 1985). This has also been the case for the Swiss Molasse basin, where the theory of deepwater waves has served as basis to successfully calculate the palaeo-water depths based on ripple-mark morphometries (Allen, J., 1984; Allen, 1981. 1997; Allen et al. 1985; Diem, 1985). Here, the focus lies on vortex ripples, which have a steepness of $h/\lambda < 0.12\text{-}0.22$ (Clifton and Dingler, 1984) or a VFI of $\lambda/h < 7.5 << 10$ (Allen, 1984) and which were likely formed by waves.

The ripple spacing λ depends on the near-bed orbital diameter d_o, which decreases exponentially with water depth (Allen, 1984, Allen, J., 1984; Miller and Komar, 1980a and 1980b; Fig. S3):

$$d_o = \lambda/0.65 \quad (1).$$

Measurements of the grain size D allow calculations of the critical velocity for sediment entrainment U_t, where variations in D need to be considered (Komar and Miller, 1973):

$$For\ D < 0.5mm;\ \ {U_t}^2 = 0.21\,(d_o/D)^{1/2}\,\frac{(\rho_s - \rho_w)gD}{\rho_w} \quad (2a),$$

$$For\ D \geq 0.5mm;\ \ U_t^{\,2} = 0.46\pi\,(d_o/D)^{1/4}\,\frac{(\rho_s - \rho_w)gD}{\rho_w} \qquad (2b).$$

Here, the variables ρ_s and ρ_w denote the sediment and water densities, respectively, and g refers to the gravitational acceleration. The maximum wave period T_{max} can then be calculated using the estimates of the near-bed orbital diameter d_o and the threshold velocity U_t for sediment entrainment (Allen, 1984):

$$T_{max} = \pi d_0/U_t \qquad (3).$$

The wave period allows to calculate the deep-water wavelength L, which is independent of the water depth and bases on the wave period only (Allen, 1984):

$$L = T^2{}_{max}\frac{g}{2\pi} \qquad (4).$$

Allen (1997) suggests that orbital diameters of oscillatory water particles decrease exponentially from the surface to greater water depths, where:

$$d_y = H\exp(y\frac{2\pi}{L}) \qquad (4),$$

where d_y is the orbital diameter at a specific water depth (-y, negative term), H is the wave height, and L is the wavelength (all in m), respectively. Similar to the diameter, the maximum orbital velocity of water particles c_y also decreases with water depth (Allen, 1997):

$$c_y = A\,\frac{2\pi}{L}c_{y=0}\exp(y\frac{2\pi}{L}) \qquad (5),$$

where A is the amplitude equal to the half of the waveheight H and $c_{y=0}$ is the celerity (wave propagation velocity in m/s) of deep-water waves at the surface, respectively (Fig. S3). According to Allen (1984) the celerity at the surface ($c_{y=0}$) can be calculated through:

$$c_{y=0} = \sqrt{\frac{gL}{2\pi}} = \frac{L}{T}. \qquad (6).$$

Since A in Eq. (5) refers to the half of the waveheight H, we can substitute A with $H/2$. Note, that at the surface, the form of deep-water waves is not expressed as perfect semicircles in height and diameter. This is particularly the case for shallow marine environments where the waves show a flattened, elliptical shape, which reduces the height of A and eventually elongates the diameter d_0 (Fig. S3, Clifton and Dingler, 1984). We further consider the relationships between waveheight H and wavelength L, which can be expressed through the height to length ratio $H/L = 0.142$ (Mitchell, 1893). By replacing H with $0.142*L$ and substituting $c_{y=0}$ with L/T Eq. (5) changes to:

$$c_y = \frac{0.142\,L}{2} * \frac{2\pi}{L} * \frac{L}{T} * \exp(y\frac{2\pi}{L}) = 0.142\,\pi\,\frac{L}{T}\exp(y\frac{2\pi}{L}) \quad (7).$$

The water depth y can then be calculated using U_t as proxy for c_y, and through the combinations of Eq. (3) and Eq. (7). This results in an expression, where the water depth y for a wave with a length L can be estimated. Since our approach mainly involves threshold conditions and maximum values, the water depth will be overestimated. Accordingly, Eq. (8) returns maximum value for palaeo-water depth:

$$y = \frac{L}{2\pi} * \ln(\frac{d_0}{0.142*2*L}) \quad (8).$$

We thus measured the ripple-spacing (λ, crest to crest), the ripple-height (h, trough to crest) and the median grain size (D) in the field. We tested whether the ratio-values of the ripple-steepness h/λ (Sleath, 1976; Miller and Komar, 1980a; Clifton and Dingler, 1984) and inversely, the ripple-index or the vertical from index VFI (Allen, 1984; Allen, J. 1979), fulfilled the criteria for vortex ripples. We then applied Eq. (9) to these 12 measurements of ripple-marks at the different sections. We justify the selection of deep-water wave theories because we focussed on those oscillatory ripple-marks (Sos-facies), which were formed in the lower shoreface (see section 4.2) where related conditions are likely to apply. The results revealed changes in bathymetrical conditions through time which were used to reconstruct the ancient sea conditions in the Molasse basin.

1.2 Estimations of palaeo-water depth from set-thickness

We use the set-thickness of preserved sedimentary bedforms to estimate the palaeo-water depth conditions during deposition of the OMM. To this extent, we mainly focus on cross-bedded- (Sc, Sct_a) and trough cross-bedded-sandstones (Sct_r) since these facies assemblages are commonly found in the OMM-deposits and they have intensely been investigated in the past by several authors (e.g. Allen, J. 1982; 1984; Allen, 1984; Rust and Gibling, 1990; Nicholson, 1993; Bridge and Tye, 2000; Mohrig et al., 2000; Leclair and Bridge, 2001; Tjerry and Fredsøe, 2005; Hajek and Heller, 2012; Blondeaux and Vittori, 2016). We use the fact, that according to these authors the bedform thickness h_b and the mean water depth y_m are positively correlated to each other. Furthermore, in the case of tabular cross-beds (Sct_a), which we interpret as sandwaves, the water depth during their formation is directly proportional to their height (e.g. Blondeaux and Vittori, 2010). In this case, the properties of sandwaves explored by Yalin (1964; 1992) returned a relationship between the mean water depth (y_m) and the mean height of the sandwave (h_b) of approximately $y_m/h_b = 6$. Values proposed by Yalin (1964) and Allen (1982; 1984), who both stated that set-thickness is increasing with water depth, resulted in the relation of $h_b/y_m = 0.1$ *to* 0.167, however with a large scatter of the plotted data. We note, however, that other authors (e.g. Stride, 1970) contested the statement that there is a correlation between the height of sandwaves and the mean water depth. In addition, Flemming (2000) also refuted the inference that the bedform height is only depending on the water depth. Instead he showed that grain-size and flow-velocity also plays a primary role in the formation of sandwaves with various heights. Nevertheless, it is possible to estimate minimum water depth levels by considering the thickness of set-heights, because the minimum water depth must be at least as high as the preserved set-thickness. We thus proceeded following the approach by Bridge and Tye (2000), who explored sandy river dunes where the sedimentary properties are similar to those of marine sandwaves (e.g. Allen, J. 1984; Hulscher, 2005) encountered in our sections. These authors proposed that the relationship between the mean water depth and mean dune height ranges in average between 6 and 10 (Bridge and Tye, 2000), which is confirmed by the study of Leclair and Bridge (2001). In addition, we need to consider that these relationships do not include post-depositional erosion or compaction of the bedforms, which accordingly results in an underestimation of the palaeo-water depth.

In summary, we used the aforementioned relationships in order to estimate the range of the paleo-water depth (y_m) from the preserved set-height (h_b) of cross-beds (Sc) and dunes (Sct_a, Sct_r) by applying the relationship of Allen (1982) and Bridge and Tye (2000), which are summarized in Eq. (1) and Eq. (2), alternatively:

$$y_{m1} = h_b / 0.1 \ to \ 0.167 \qquad \text{after Allen (1982)} \qquad (1),$$

$$y_{m2} = h_b * 6 \ to \ 10 \qquad \text{after Bridge and Tye (2000)} \qquad (2).$$

The results of our palaeo-bathymetric estimations are presented as plots in the sedimentological profile sections (Figs. 5). Calculations of cross-beds thickness of inferred sand-waves are shown table 1 together with already published data from the Swiss Molasse basin (Table 2).

References

Allen, J.R.L. : A model for interpretation of wave ripple-marks using their wavelength, textural composition, and shape. J. geol. Soc. London, 146. 673 – 682, 1979.

Allen, J.R.L. : Sedimentary Structures. Their Characteristics and Physical Basis. Vol. I. Developments in Sedimentology 30A. Elsevier, Amsterdam, 593 p., 1982.

Allen, J.R.L. : Sedimentary Structures. Their Characteristics and Physical Basis. Vol. I. Developments in Sedimentology 30B. Elsevier, Amsterdam, 679 p., 1984.

Allen, P.A. : Earth Surface Processes, 404 p. ISBN 0-632-03507-2, 1997.

Allen, P.A. : Some Guidelines In Reconstructing Ancient Sea Conditions From Wave Ripplemarks. Marine Geology, 43, 59 – 67, 1981.

Allen, P.A. : Reconstruction of ancient sea conditions with an example from the Swiss Molasse. Marine Geology 60, 455 – 473, 1984

Allen, P. A., and Homewood, P. : Evolution and mechanics of a Miocene tidal sandwave. Sedimentology, 31 (1), 63 – 81, 1984.

Allen, P.A., Mange-Rajetky, A. and Matter, A. : Dynamic palaeogeography of the open Burdigalian seaway, Swiss Molasse basin. Eclogae Geologicae Helvetia 78, 351 – 381, 1985.

Allen, P. A. and Hoffman, P. F. : Extreme winds and waves in the aftermath of a Neoproterozoic glaciation. Nature, 433 (7022), 123 p., 2005.

Baas, J. H. : Ripple, ripple mark, ripple structure. In: Sedimentology. Encyclopedia of Earth Science, Springer, Berlin, Heidelberg, 921 – 925, 1978.

Blondeaux, P. and Vittori, G. : A model to predict the migration of sand waves in shallow tidal seas. Continental Shelf Research, 112, 31 – 45, 2016.

Bridge, J.S. and Tye, R.S. : Interpreting the dimensions of ancient fluvial channel bars, channels and channel belts from wireline-logs and cores. AAPG Bulletin, 84 (8), 1205 – 1228, 2000.

Clifton, H.E. and Dingler, J.R. : Wave-Formed Structures and Paleoenvironmental Reconstruction. Marine Geology, 60, 165 – 198, 1984.

Daidu, F., Yuan, W. and Min, L. : Classifications, sedimentary features and facies associations of tidal flats. Journal of Palaeogeography, 2 (1), 66 – 80, 2013.

Dam, G., and Andreasen, F. : High-energy ephemeral stream deltas; an example from the Upper Silurian Holmestrand Formation of the Oslo Region, Norway. Sedimentary Geology, 66 (3-4), 197 – 225, 1990.

Diem, B. : Analytical method for estimating paleowave climate and water depth from wave ripple marks. Sedimentology, 32, 705 – 720, 1985.

Diem, B. : Die Untere Meeresmolasse zwischen der Saane (Westschweiz) und der Ammer (Oberbayern). Eclogae Geologicae Helvetiae, 79 (2), 493 – 559, 1986.

Flemming, B. : The role of grain size , water depth and flow velocity as scaling factors controlling the size of subaqueous dunes. Marine Sandwave Dynamics, 23 & 25, 55 – 61, 2000.

Frieling, D., Mazumder, R., and Reichenbacher, B. : Tidal sediments in the Upper Marine Molasse (OMM) of the Allgäu area (Lower Miocene, Southwest-Germany). Neues Jahrbuch für Geologie und Paläontologie-Abhandlungen, 254 (1-2), 151 – 163, 2009.

Hajek, E.A. and Heller, P.L. : Flow-Depth Scaling In Alluvial Architecture and Nonmarine Sequence Stratigraphy: Example from the Castlegate Sandstone, Central Utah, U.S.A. Journal of Sedimentary Research, 82 (2), 121 – 130, 2012.

Hulscher, S.J.M.H. and Dohmen-Janssen, C.M. : Introduction to special section on Marine Sand Wave and River Dune Dynamics. Journal of Geophysical Research, 110, 1 – 6, 2005.

Jost, J., Kempf, O. and Kälin, D. : Stratigraphy and palaeoecology of the Upper Marine Molasse (OMM) of the central Swiss Plateau. Swiss Journal of Geosciences, 109(2), 149 – 69, 2016.

Keller, B. : Fazies und Stratigraphie der Oberen Meeresmolasse (Unteres Miozän) zwischen Napf und Bodensee. Ph.D., Bern, 302 p., 1989.

Keller, B. : Wirkung von Wellen und Gezeiten bei der Ablagerung der Oberen Meeresmolasse–Löwendenkmal und Gletschergarten–zwei anschauliche geologische Studienobjekte. Mitteilungen der Naturforschenden Gesellschaft Luzern, 31, 245 – 271, 1990.

Komar, P.D. and Miller, M.C. : The threshold of sediment movement under oscillatory water waves. 43 (4), 1101 – 1110, 1973.

Leclair, S.F. and Bridge, J.S. : Quantitative interpretation of sedimentary structures formed by river dunes. Journal of Sedimentary Research, 71, 713 – 716, 2001.

Miall, A. D. : The Geology of Fluvial Deposits. Sedimentary Facies, Basin Analysis, and Petroleum Geology. Springer. 582 p., 1996.

Michell, M.A. : The highest Waves in Water. The London, Edinbrugh, and Dublin Philosophical Magazine and Journal of Science, 36 (5), 430 – 437, 1893.

Miller, M.C. and Komar, P.D. : Oscillation Sand Ripples Generated by Laboratory Apparatus. Journal of Sedimentary Research, 50(1), 173 – 182, 1980a.

Miller, M.C. and Komar, P.D. : A field investigation of the relationship between oscillation ripple spacinng and the near-bottom water orbital motions. Journal of Sedimentary Research, 50 (1), pp.183 – 191, 1980b.

Mohrig, D., Heller, P.L., Paola, C. and Lyons, W.J. : Interpreting avulsion process from ancient alluvial sequences: Guadalope-Matarranya system (northern Spain) and Wasatch Formation (western Colorado). GSA Bulletin, 112 (12), 1787 – 1803, 2000.

Nicholson, P.G. : A basin reappraisal of the Proterozoic Torridon Group, northwest Scotland. Spec. Publs. Int. Ass. Sediment 20, 183 – 202, 1993.

Nichols, P.G. : Sedimentology & Stratigraphy. Blackwell Sci., 355 p., 1999.

Platt, N. H. and Keller, B. : Distal alluvial deposits in a foreland basin setting—the Lower Freshwater Miocene), Switzerland: sedimentology, architecture and palaeosols. Sedimentology, 39 (4), 545 – 565, 1992.

Reineck, H.E. and Singh, I. B. : Depositional sedimentary environments. Springer, 549 p., 1980.

Rust, B.R. and Gibling, M.R. : Braidplain evolution in the Pennsylvanian South Bar Formation, Sydney basin, Noca Scotia, Canada. Journal of Sedimentary Petrology, 60 (1), 59 – 72, 1990.

Shanmugam, G. : Deep-marine tidal bottom currents and their reworked sands in modern and ancient submarine canyons. Marine and Petroleum Geology, 20 (5), 471 – 491, 2003.

Schlunegger, F., Leu, W. and Matter, A. : Sedimentary Sequences, Seismic Facies, Subsidence Analysis, and Evolution of the Burdigalian Upper Marine Molasse Group, Central Switzerland. The American Association of Petroleum Geologists 81, 1185 – 1207, 1997.

Sleath, J.F.A. : On rolling grain ripples. J. Hydraul. Res., 14, 69 – 80, 1976.

Stride, A. H. : Shape and size trends for sandwaves in a depositional zone of the North Sea. Geol. Mag. 107, 469 – 477, 1970.

Tanner, W.F. : Numerical estimates of ancient waves, water depth and fetch. Sedimentology, 16, 71 – 88, 1971.

Tjerry, S. and Fredsøe, J. : Calculation of dune morphology. Journal of Geophysical Research, 110, 13 p., 2005.

Yalin, M.S. : River Mechanics. Pergamon Press, Oxford, 219 p., 1992.

Yalin, M.S. : Geometrical properties of sand waves. Journal of the Hydraulics Division, ASCE, 90, 105 – 119, 1964.

Table S1: Lithofacies types

Abbr.	*Lithofacies types*	*Bedforms and inferred processes*	*References (e.g.)*
G-	*Conglomerates*	*Grains > 2 mm in diameter*	-
S-	*Sandstones*	*Grains between 0.063 and 2 mm in diameter (fine- to coarse-grained; fS, mS, cS)*	-
M-	*Silt- and mudstones*	*Particles < 0.063 mm in diameter (Silt & Clay fraction)*	-
Gc	Cross-bedded	Deposits within a braided river system, mainly at the confluence between a tributary and a main channel; formed by fluvial processes	Platt and Keller, 1992
Gm	Massive-bedded	Deposits within a braided river system, mainly within the main channel; formed by fluvial processes	Platt and Keller, 1992; Schlunegger et al., 1997;
Sbr	Branching-ripple marks	Deposits within a wave-dominated coast under shallow water conditions; formed by waves	Allen, 1984
Sc	Cross-bedded	Deposits of sand-reefs, backshore channels, in combination with Gp: Gilbert-delta deposits; in combination with Sm: Crevasse splays; formed by fluvial or wave-dominated processes	Allen, 1982; 1984; Rust and Gibling, 1990
Scc	Calcareous cross-beds	Deposits within an offshore environment, representing an assemblage of Sc, Shf + coquinas and Sg; these tabular-crossbeds (Sct_a) formed by strong tidal currents	Allen et al., 1985
Sce	Epsilon cross-bedded	Deposits in tidal channels, sigmoidal laminae mark slip faces of meanders; formed by tidal-dominated (if marine) & fluvial processes (if terrestrial)	Frieling et al., 2009
Scr	Current-ripple marks	Deposits in shallow bathymetrical conditions due to currents; asymmetric ripples show shallow stoss- and steep lee-side, separated mostly by truncated crests; formed by tidal-dominated processes	Baas, 1978
Sct_a	Tabular cross-bedded	Deposits of (mega-) sand-waves within a subtidal environment, in combination with Scr and Md at the base of lamina sets; formed by strong tidal currents	Reineck and Singh, 1980; Allen, 1982; Allen and Homewood, 1984; Yalin, 1964
Sct_r	Trough cross-bedded	Deposits of subtidal-shoals, in combination with Scr and Md at the base of the throughs; Deposits of distal mouth-bars or tidal inlets, in combination with Sm; formed by tidal-dominated & fluvial processes	Allen and Homewood, 1984
Sf	Bioturbation, fossil tracks	Organism tracks within a sand-flat, or alternatively within subtidal conditions, in relation to a	Nichols, 1999

		tidal-dominated environment; Sf mark the presence of endobenthic organisms	
Sg	Pebbly-lag within sandstones	Deposits within a Gilbert-delta, visible on top-, fore- and bottom-sets or alternatively as storm-deposits due to high-energetic waves; formed by fluvial & wave-dominated processes	Miall, 1996
Shf	Shell fragments	Deposits of shell-fragments, mostly in combination with sandstones; recording the occurrence of too high-energetic waves during storm events	Jost et al., 2016
Slc	Lithoclast cross-beds	Deposits similar to Scc. However, Slc-beds are void of coquinas & Shf; formed by strong tidal-currents on subtidal shoals	Jost et al., 2016
Sm	Massive-bedded	Deposits of sandstones with no distinct fabric, could either represent deposits of floodplains with crevasse-splays or, in combination with Srs, represents a period of fast sedimentation during storms; formed by fluvial or wave-dominated processes	Dam and Andreasen, 1990
Sos	Oscillating-ripple marks	Sandstone deposits, which show a distinct spacing between crests, have a characteristic height and symmetry. Often associated with Sbr-facies. These assemblages represent the occurrence of wave activities in the near-shore.	Reineck and Singh, 1980; Clifton and Dingler, 1984; Miller and Komar, 1980a
Sp	Parallel-laminated (or parting-/transcurrent lineation)	Deposits within the surf-and-swash zone near the wet-beach during shallow water conditions, sequences are mostly normally graded; formed by swash and back-swash of water in response to wave-dominated processes	Keller, 1990
Srs	Ridge-and-swale structures (or tempestites)	Deposits by high-energetic waves during storms, sometimes in combination with Gp	Diem, 1986
Sv	Volcanoes (dewatering structures)	Dewatering structures, which formed in response to fast overburden of water-saturated sediments; formed by fluvial or wave-dominated processes	Allen et al., 1985
Mcl	Climbing-ripple marks	Fast sedimentation within decelerating flows of silt and possibly fS; formed during an abrupt decrease of wave-activities or by tidal-dominated processes during incipient ebb-stage	Allen and Hoffman, 2005
Md	Draping / mud-drape	Deposits of slack water stages between ebb and tide within a tidal-dominated environment, or alternatively sedimentation from a standing water in wave-protected areas; possible deposits within the backshore of a coast	Shanmugam, 2003
Mf	Bioturbation, fossil tracks	Fossil tracks within a tidal-flat, destructive in combination with Mp, resulting in Mm-structures with exichnias; formed during ebb-tide where Mf mark the presence of endobenthic organisms	Dam and Andreasen, 1990
Mfl	Flaser-bedding	Amount of sand > amount of mud, generating isolated mud-drapes on top of ripple crests and in ripple-depressions (troughs); formed by periodic current, where mud-drapes are formed during slack water stage	Keller, 1989; Daidu et al., 2013

Mle	Lens-bedding; lenticular-bedding	Amount of mud > amount of sand; sand is visible as isolated lenses; truncated crests mark the presence of erosive currents; formed by tidal currents on a tidal-flat or within deeper bathymetrical conditions	Keller, 1989
Mm	Massive-bedded	Muddy-layers with no distinct fabric, mostly in combination with Mf and root-casts, alternatively Mm mark floodplain deposits; formed during slack water stages by tidal-processes or by fluvial-processes through flooding on a floodplain	Miall, 1996
Mp	Parallel-lamination	Stratified muddy-layers, often in combination with and root-casts and mottled colours, which indicate incipient palaeosoil genesis in a backshore environment, or alternatively on floodplains of rivers; formed in a tidal or fluvial environment	Keller, 1990

Table S2: Estimates of water depths from preserved cross-bed thickness

Unit	***Site (this study; Fig. 2)***	***Water depth (this study)***	***Water depth and location (other studies)***
OMM-Ib (base)	*Sense*	*24 – 40 m*	
OMM-Ib (base)	*Entlen*	*12 – 20 m*	
c. OMM-Ib (?)	*Marly*	*12 – 20 m*	*10 m, Marly (Allen and Homewood, 1984)*
c. OMM-Ib (?)	*St. Magdalena*	*3 – 5 m*	
OMM-Ib	*Estavayer-le-Lac*	*30 – 50 m*	
OMM-Ib	*Mägenwil*	*36 – 60 m; up to 100 m in places*	*25 – 60 m, Mägenwil (Allen and Homewood, 1984)*
OMM-Ib(?)			*10 – 35 m, Bay near Napf (Keller, 1989)*
OMM-II			*20 m, Pfänder-Delta (Schaad et al., 1992)*

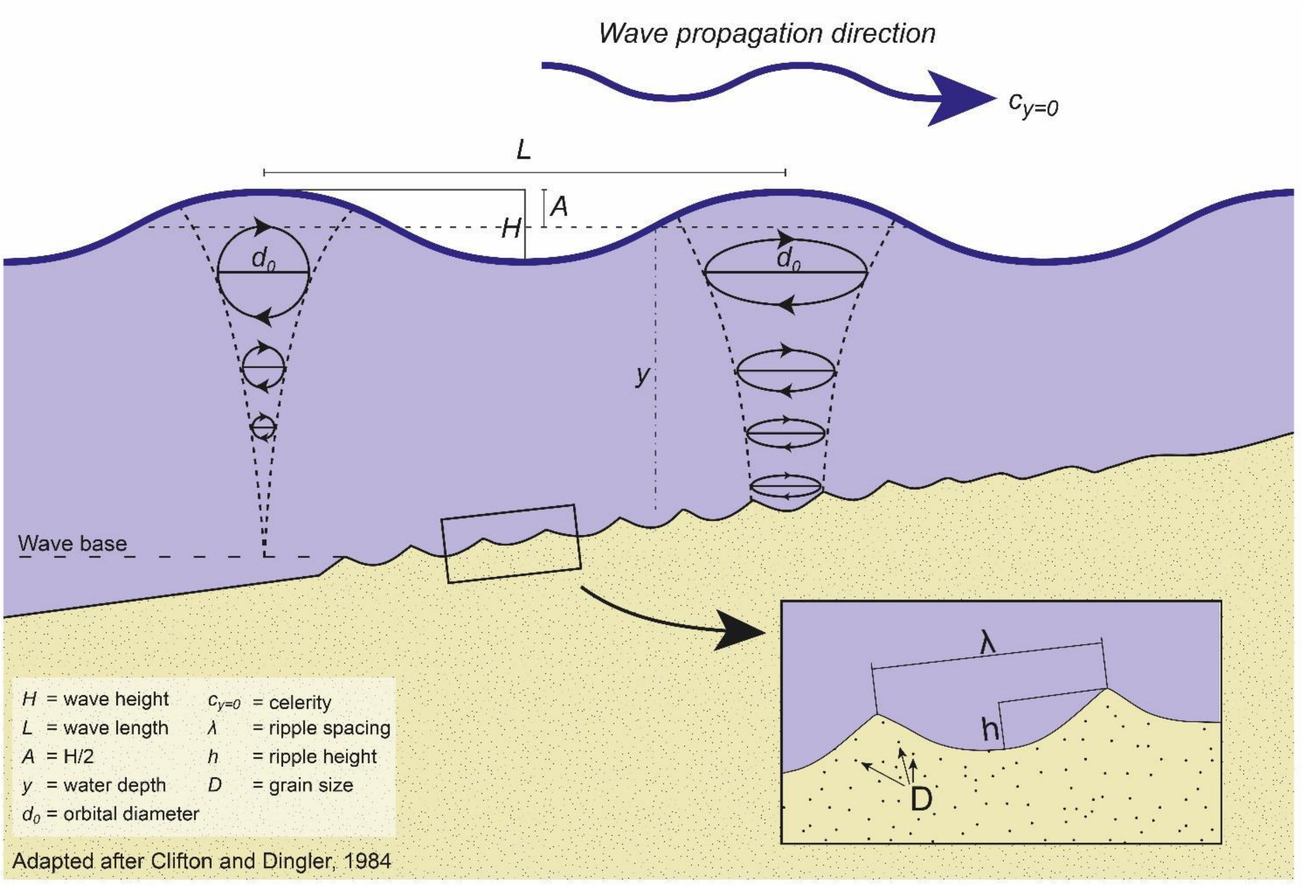

Figure S3: Schematic sketch showing important parameters of waves and wave-formed ripple marks. Note, the orbital diameter (do) refers to the wave height at the surface (H) for perfect sinusoidal shaped waves. All variables are measured in SI-units. Please see Figs. 5 for plots of the calculated water depth from oscillatory ripple-marks. Figure mod. after Clifton and Dingler, 1984.

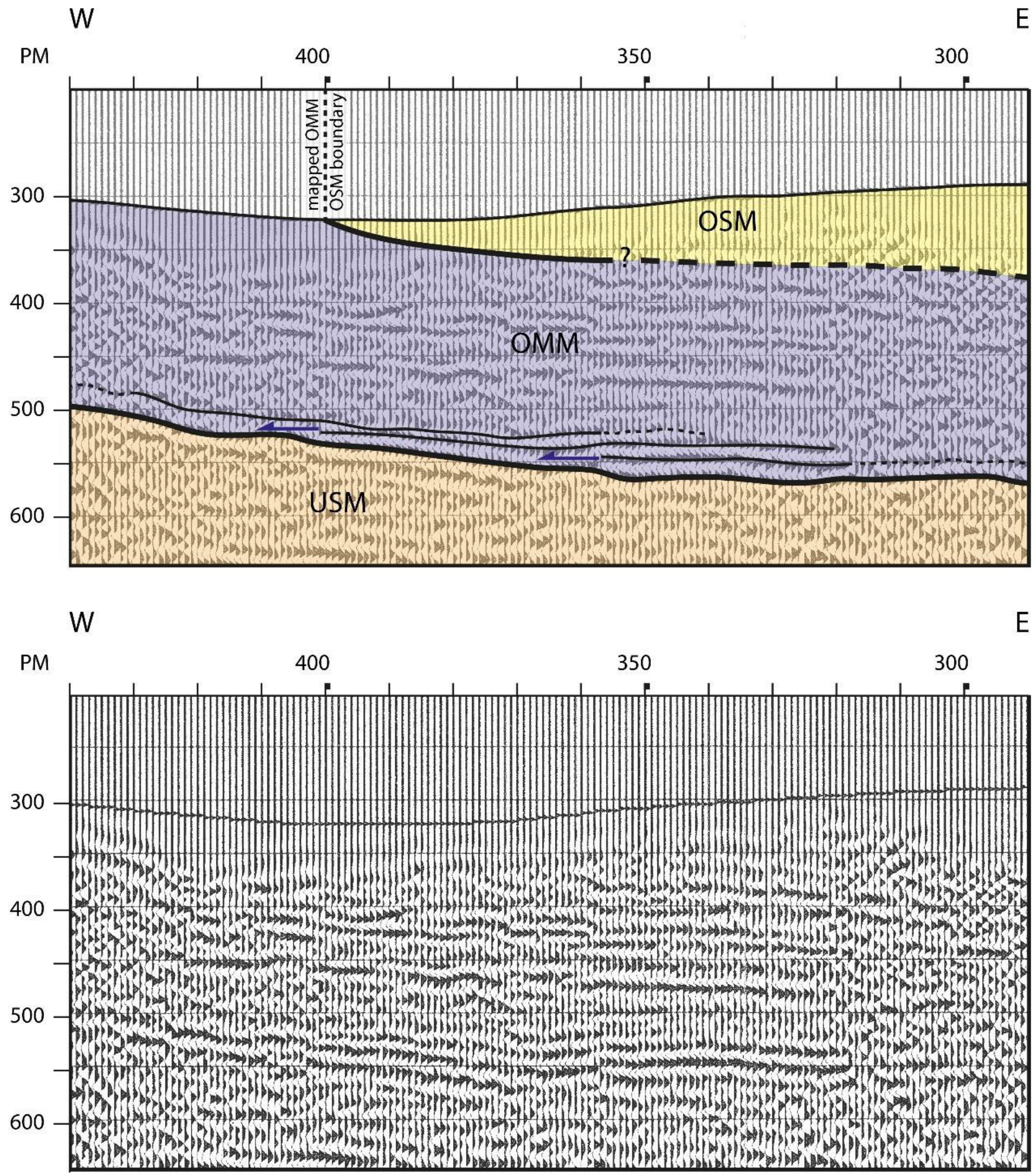

Figure S4: Seismic section BEAGBE.N780025 (courtesy SEAG, Aktiengesellschaft für Schweizerisches Erdöl, Langnau am Albis, 2019) showing the westward directed transgression of the basal OMM-deposits. Blue arrows indicate onlaps of OMM onto USM sediments. Please see Fig. 2 for trace of seismic line and see text for further discussion.

Figure S5: Photos showing the sedimentological architecture of the Gurten drillcore from top right to bottom left (courtesy Kellerhals and Haefeli AG, Geologen Bern, 2019).


UNIVERSITÄT BERN 1989
BOHRUNG
GURTEN
17
16
15
14
13
12
18
17
16
15
14
13

UNIVERSITÄT BERN 1989
BOHRUNG
GURTEN
23
22
21
20
19
18
24
23
22
21
20
19

UNIVERSITÄT BERN 1989

BOHRUNG GURTEN

UNIVERSITÄT BERN 1989

BOHRUNG GURTEN

UNIVERSITÄT BERN 1989

BOHRUNG GURTEN

UNIVERSITÄT BERN 1989

BOHRUNG GURTEN

BOHRUNG GURTEN

UNIVERSITÄT BERN 1989

53 52 51 50 49 48

54 53 52 51 50 49

BOHRUNG GURTEN

UNIVERSITÄT BERN 1989

UNIVERSITÄT BERN 1989

BOHRUNG GURTEN


UNIVERSITÄT BERN 1989
BOHRUNG
GURTEN
71
70
69
68
67
66
72
71
70
69
68
67


UNIVERSITÄT BERN 1989
BOHRUNG
GURTEN
77
76
75
74
73
72
78
77
76
75
74
73

UNIVERSITÄT BERN 1989

BOHRUNG GURTEN


BOHRUNG
GURTEN
UNIVERSITÄT BERN 1989
89
88
87
86
85
84
90
89
88
87
86
85

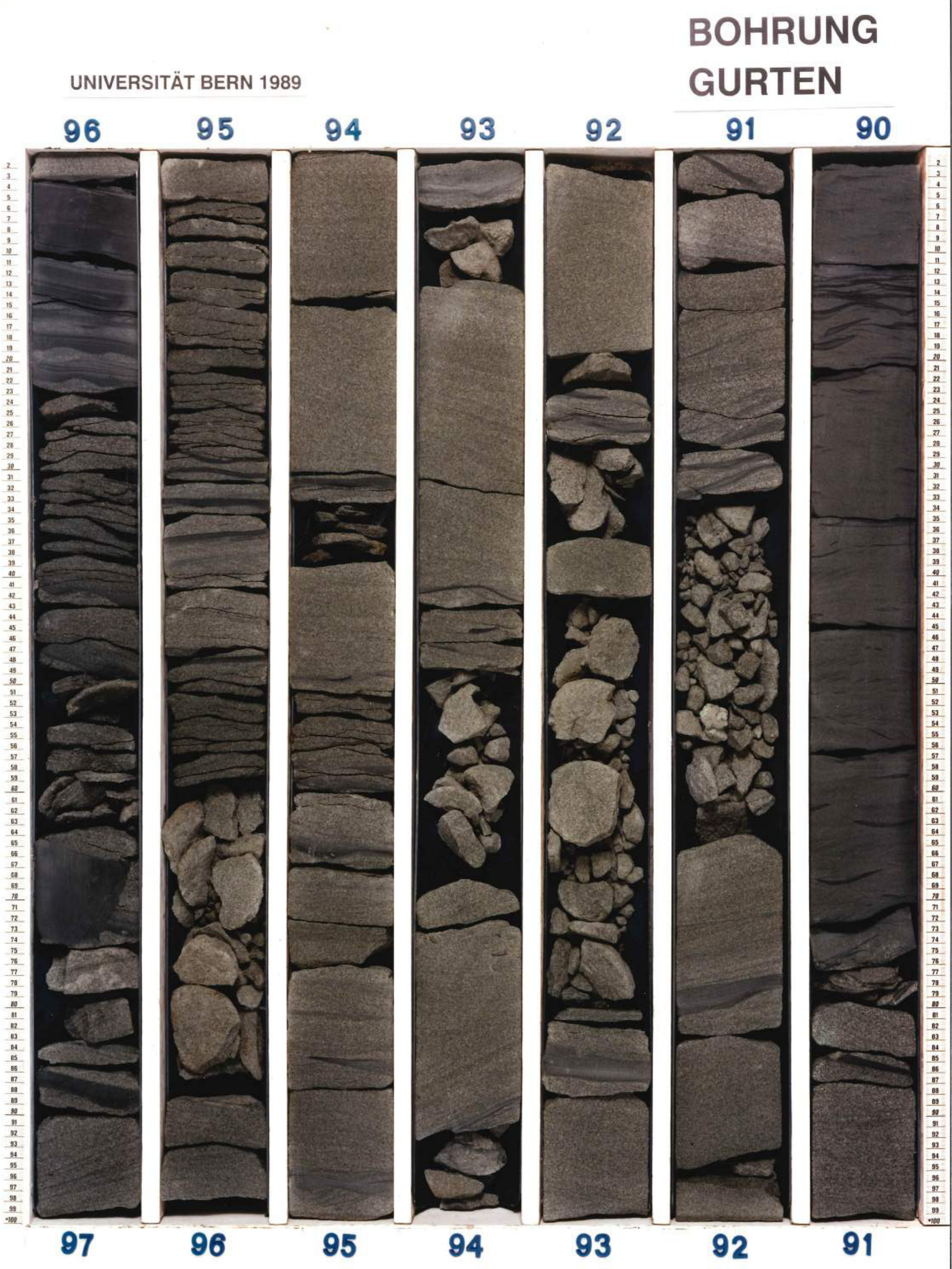

UNIVERSITÄT BERN 1989
BOHRUNG
GURTEN
96
95
94
93
92
91
90
97
96
95
94
93
92
91

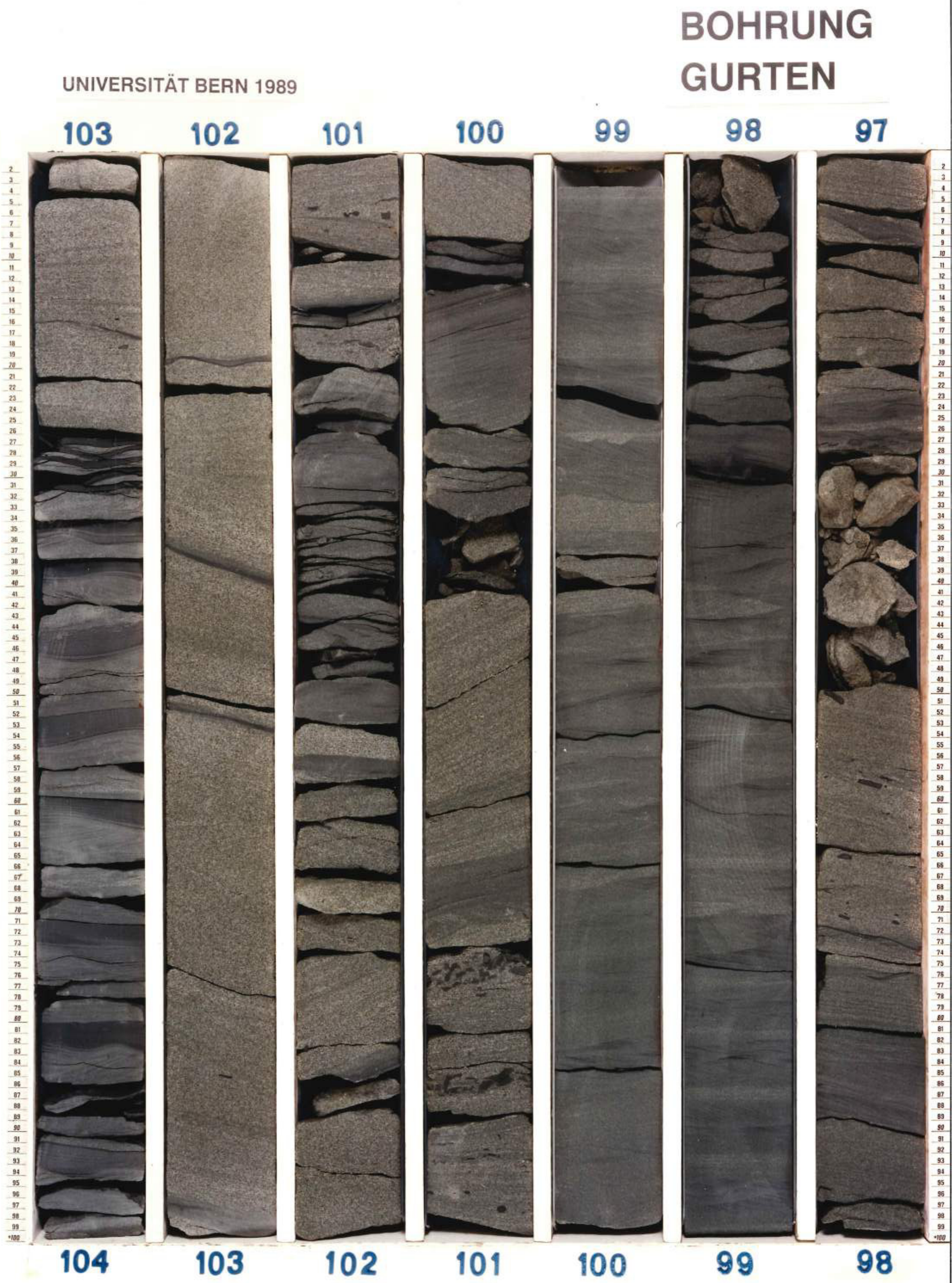
BOHRUNG
GURTEN
UNIVERSITÄT BERN 1989
103 102 101 100 99 98 97
104 103 102 101 100 99 98

BOHRUNG GURTEN

BOHRUNG GURTEN

BOHRUNG
GURTEN

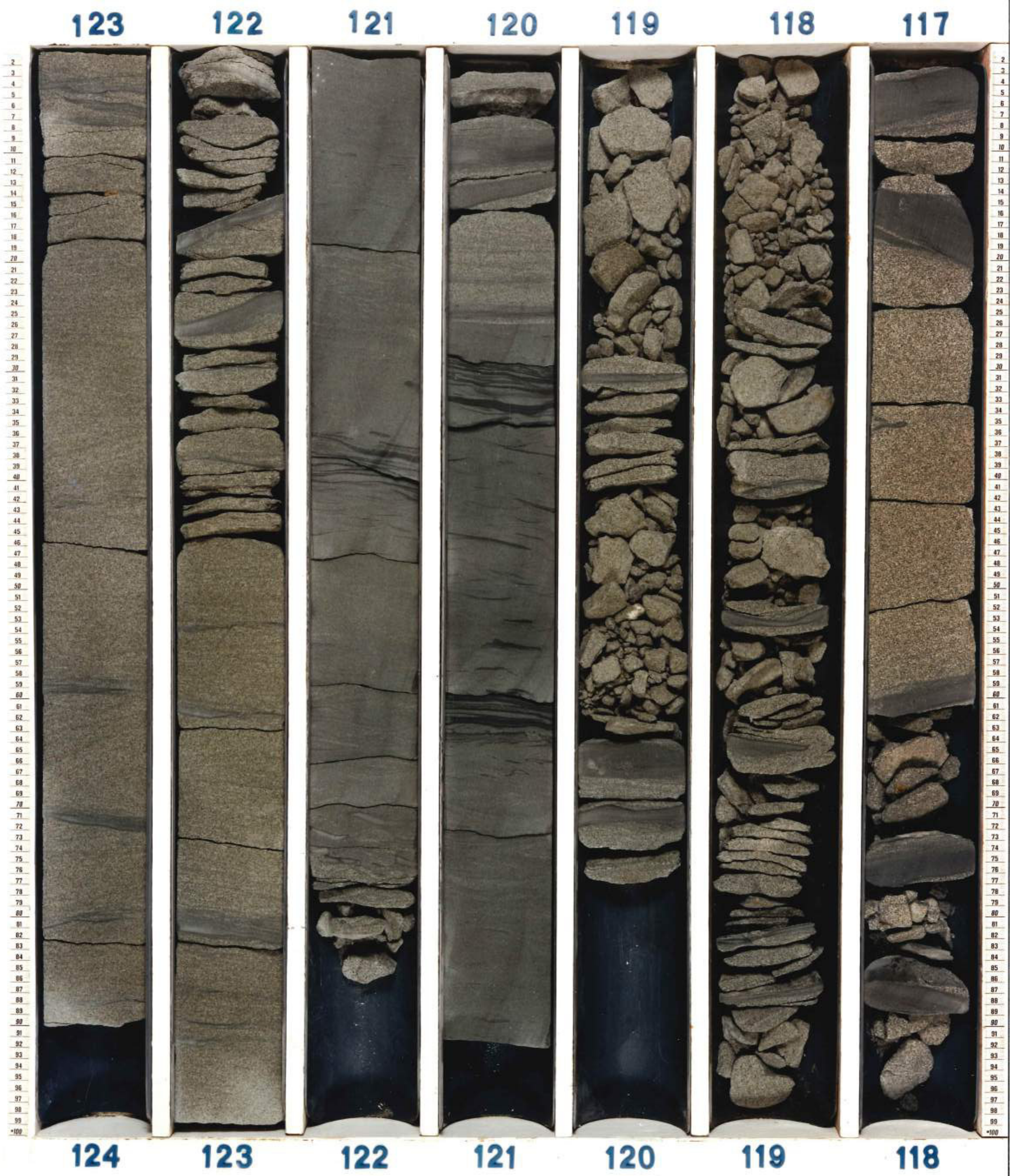

BOHRUNG GURTEN

BOHRUNG GURTEN

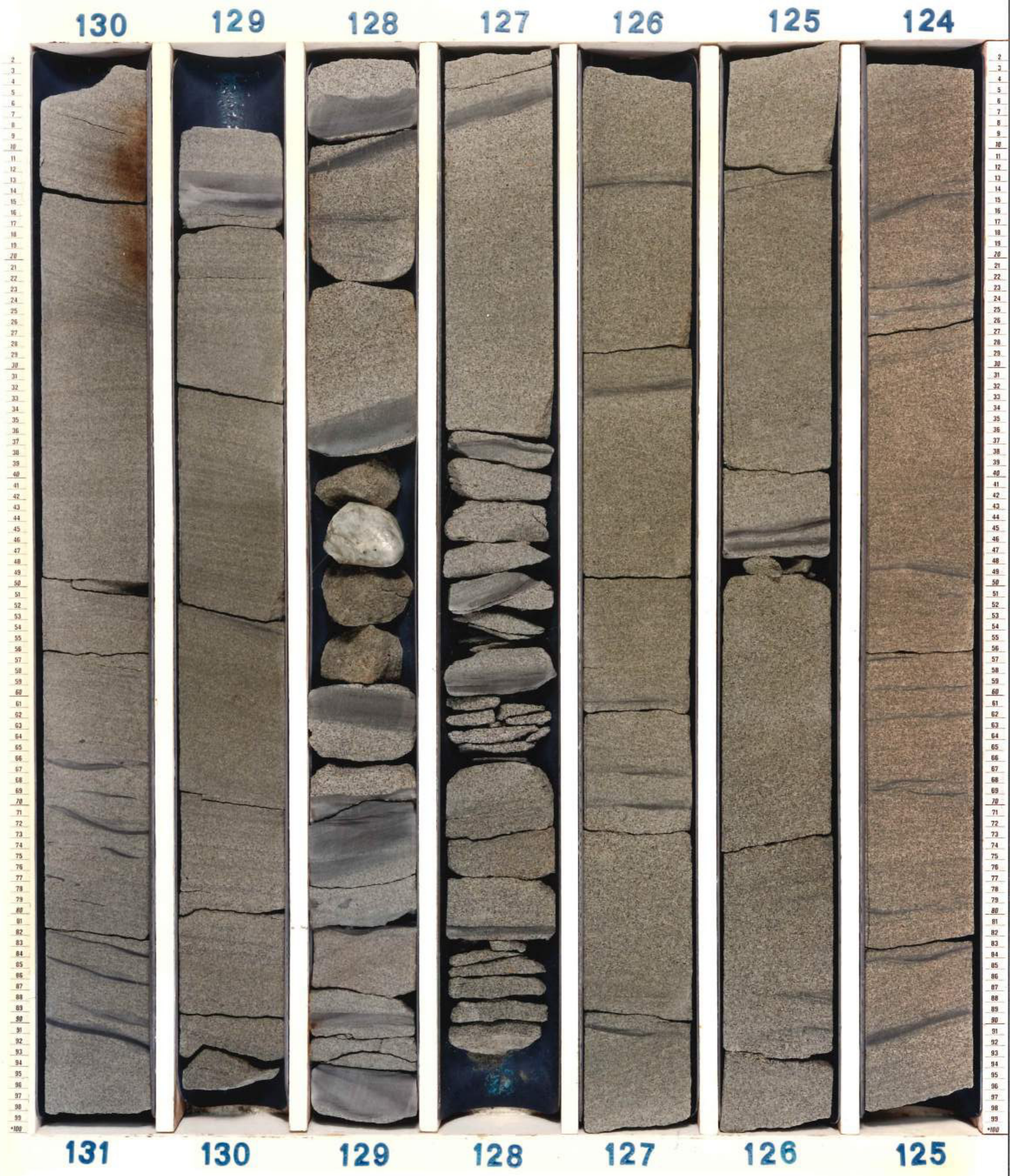

BOHRUNG GURTEN

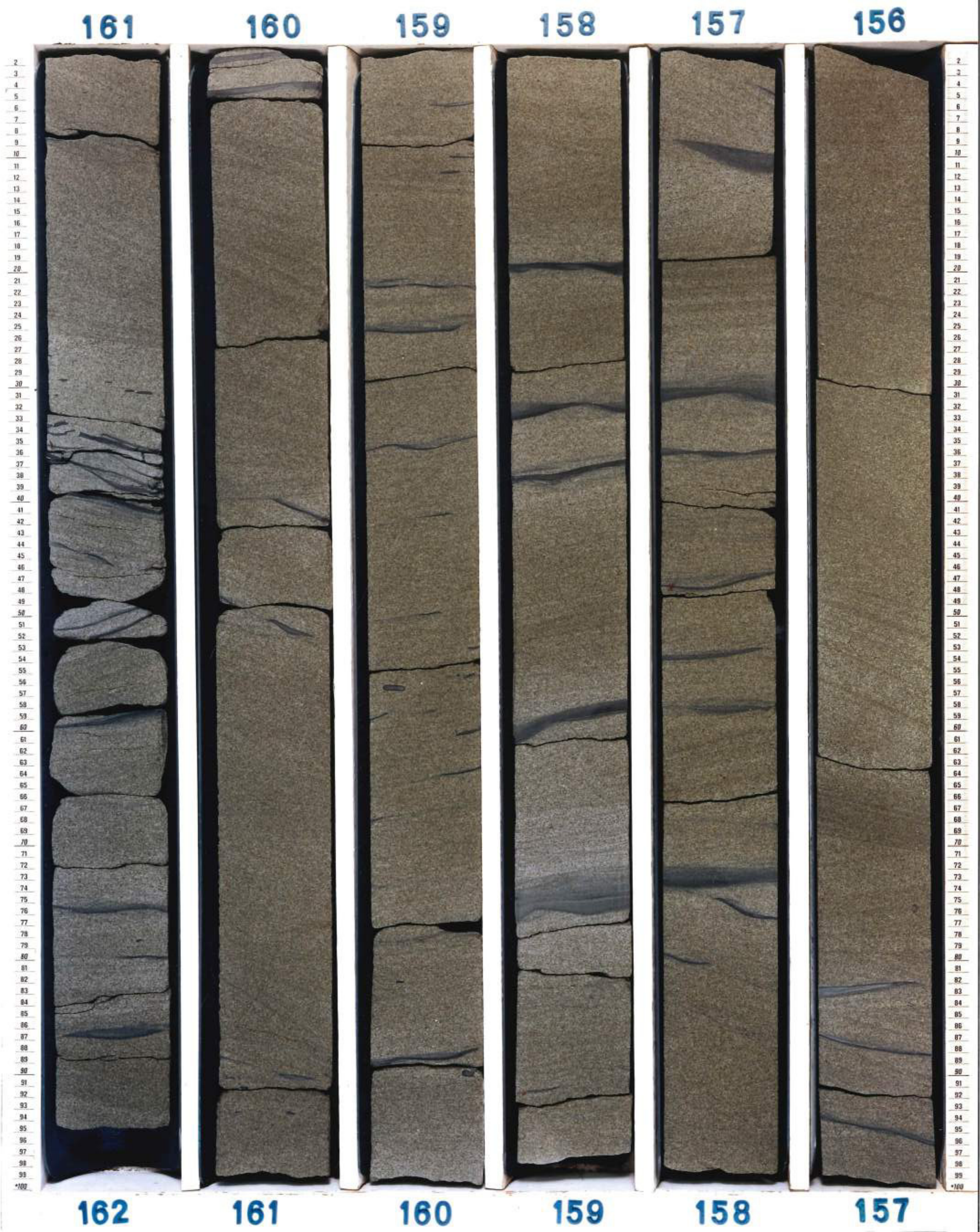

BOHRUNG GURTEN

BOHRUNG GURTEN

BOHRUNG GURTEN

BOHRUNG GURTEN

BOHRUNG
GURTEN

BOHRUNG GURTEN

BOHRUNG
GURTEN

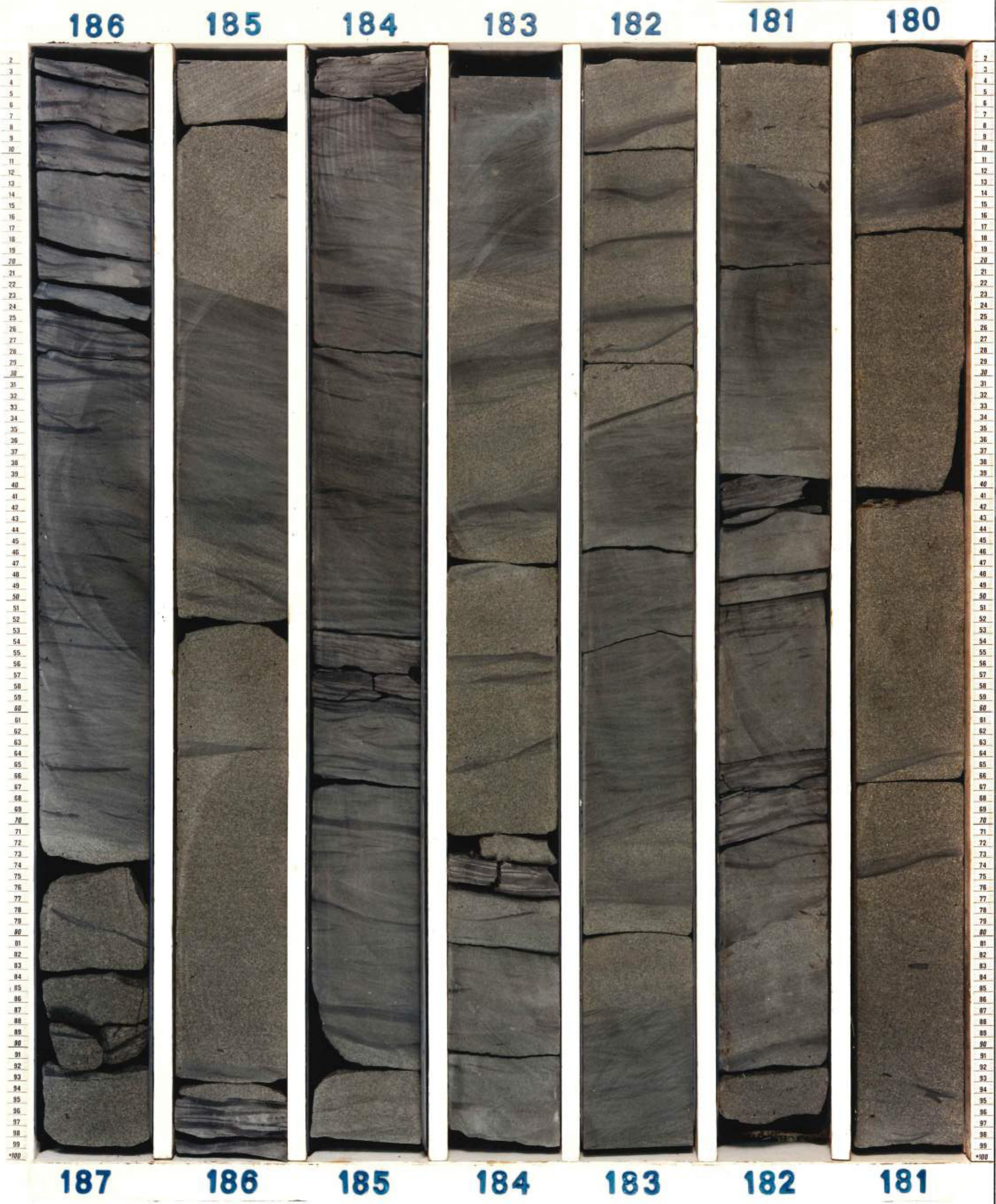


UNIVERSITÄT BERN 1989
BOHRUNG
GURTEN
193
192
191
190
189
188
187
194
193
192
191
190
189
188

UNIVERSITÄT BERN 1989

BOHRUNG GURTEN

UNIVERSITÄT BERN 1989

BOHRUNG GURTEN

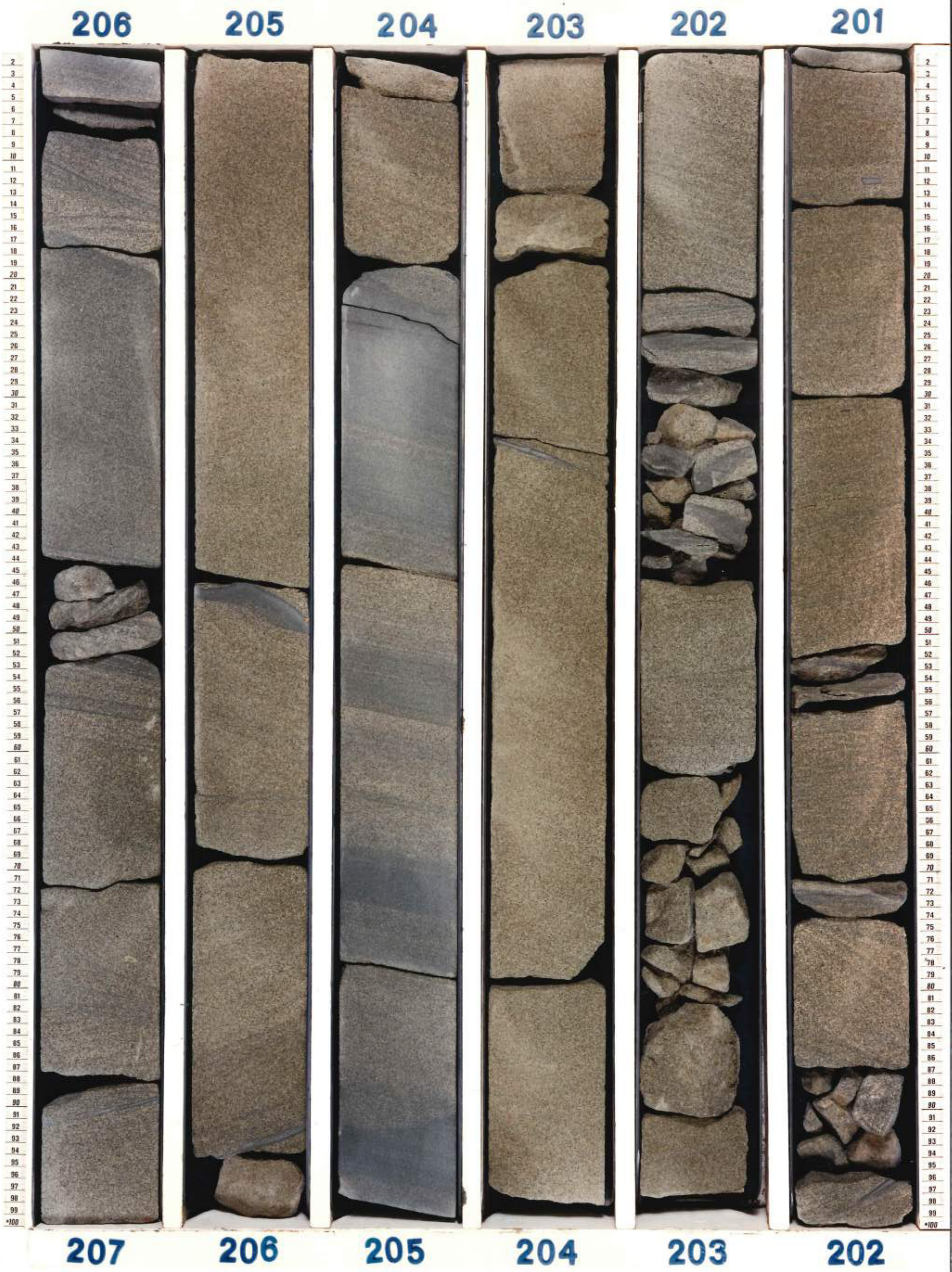

UNIVERSITÄT BERN 1989

BOHRUNG GURTEN

UNIVERSITÄT BERN 1989

BOHRUNG GURTEN

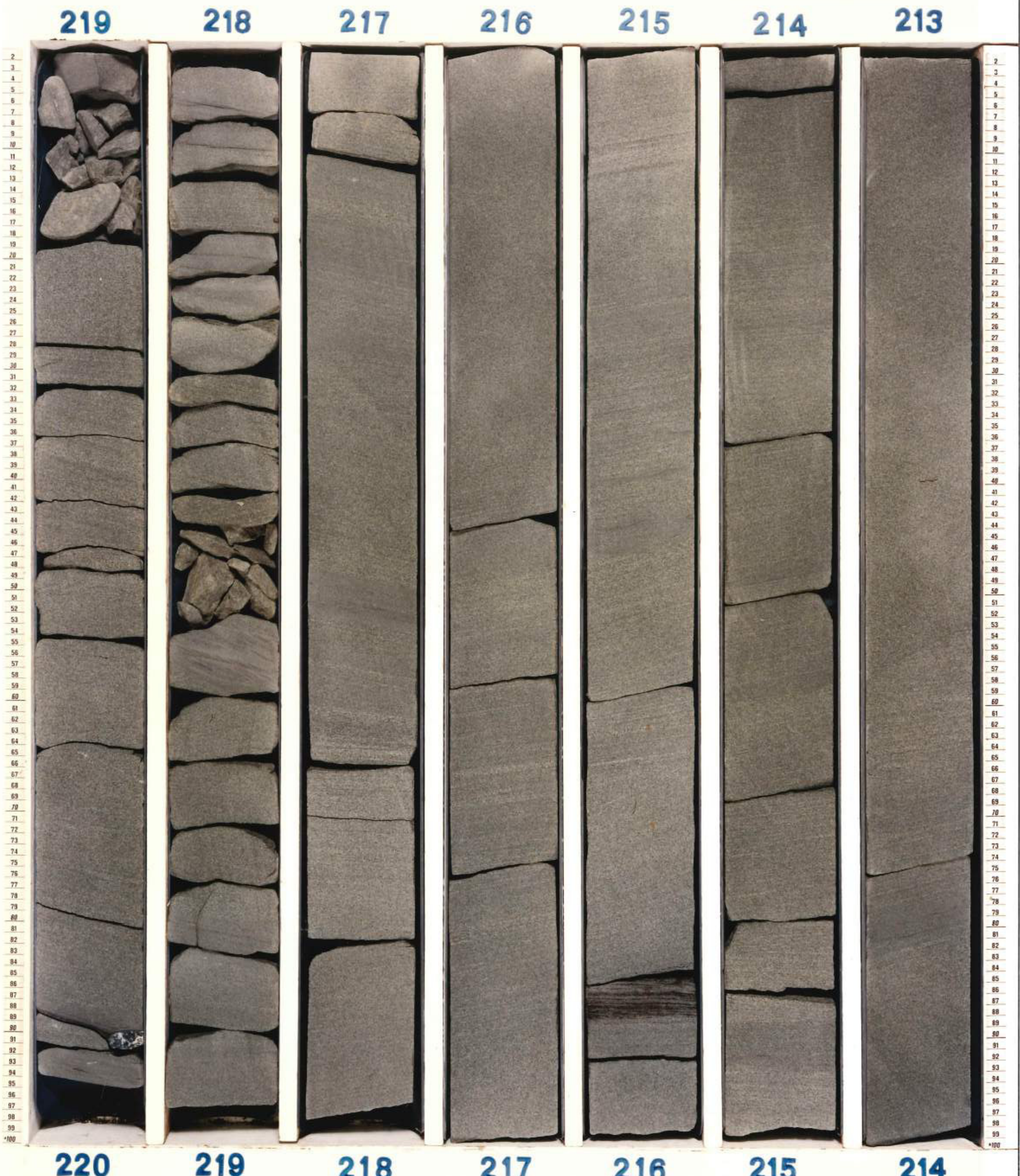

UNIVERSITÄT BERN 1989

BOHRUNG GURTEN

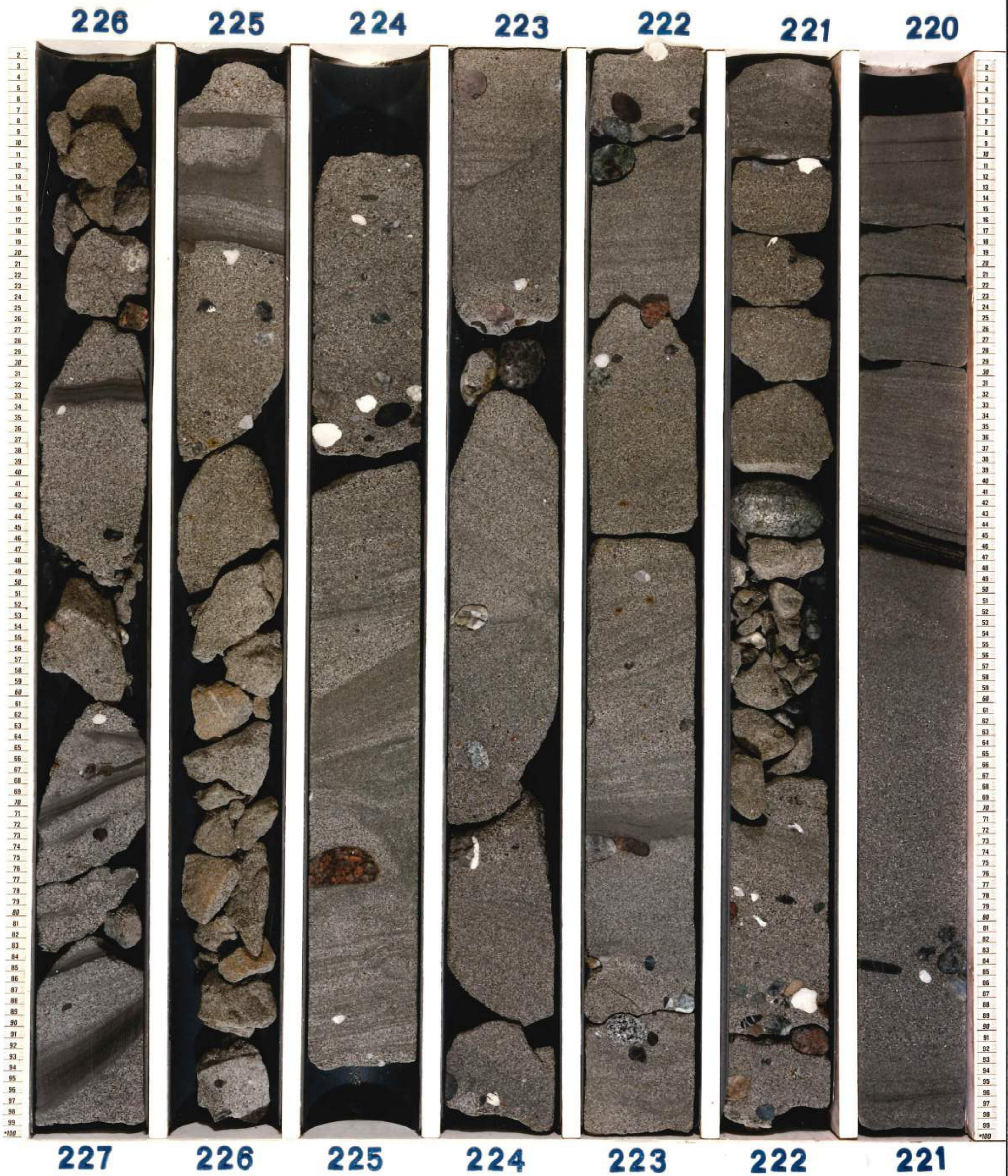


UNIVERSITÄT BERN 1989
BOHRUNG GURTEN
233
232
231
230
229
228
227
234
233
232
231
230
229
228

UNIVERSITÄT BERN 1989

BOHRUNG GURTEN

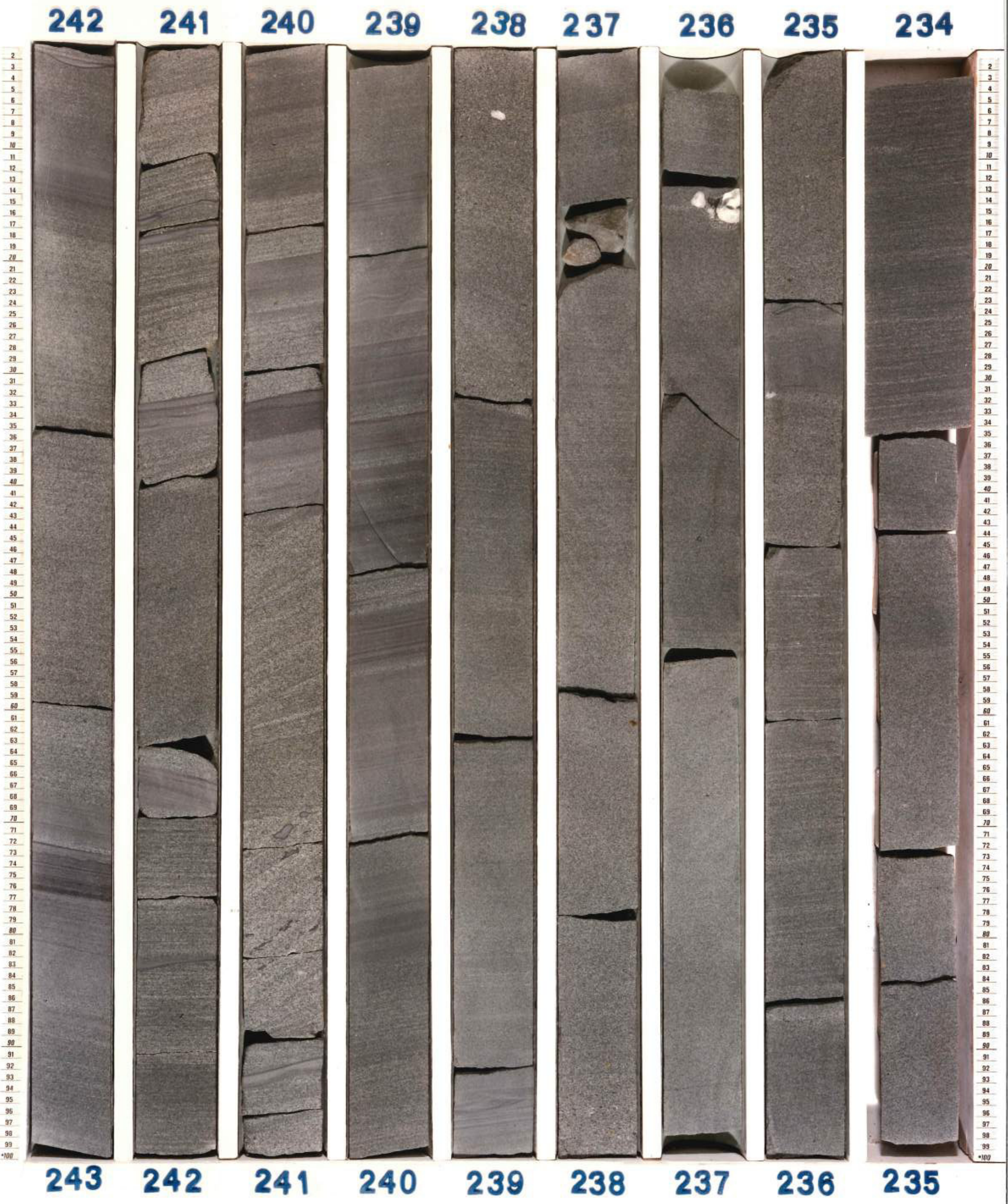

UNIVERSITÄT BERN 1989

BOHRUNG GURTEN

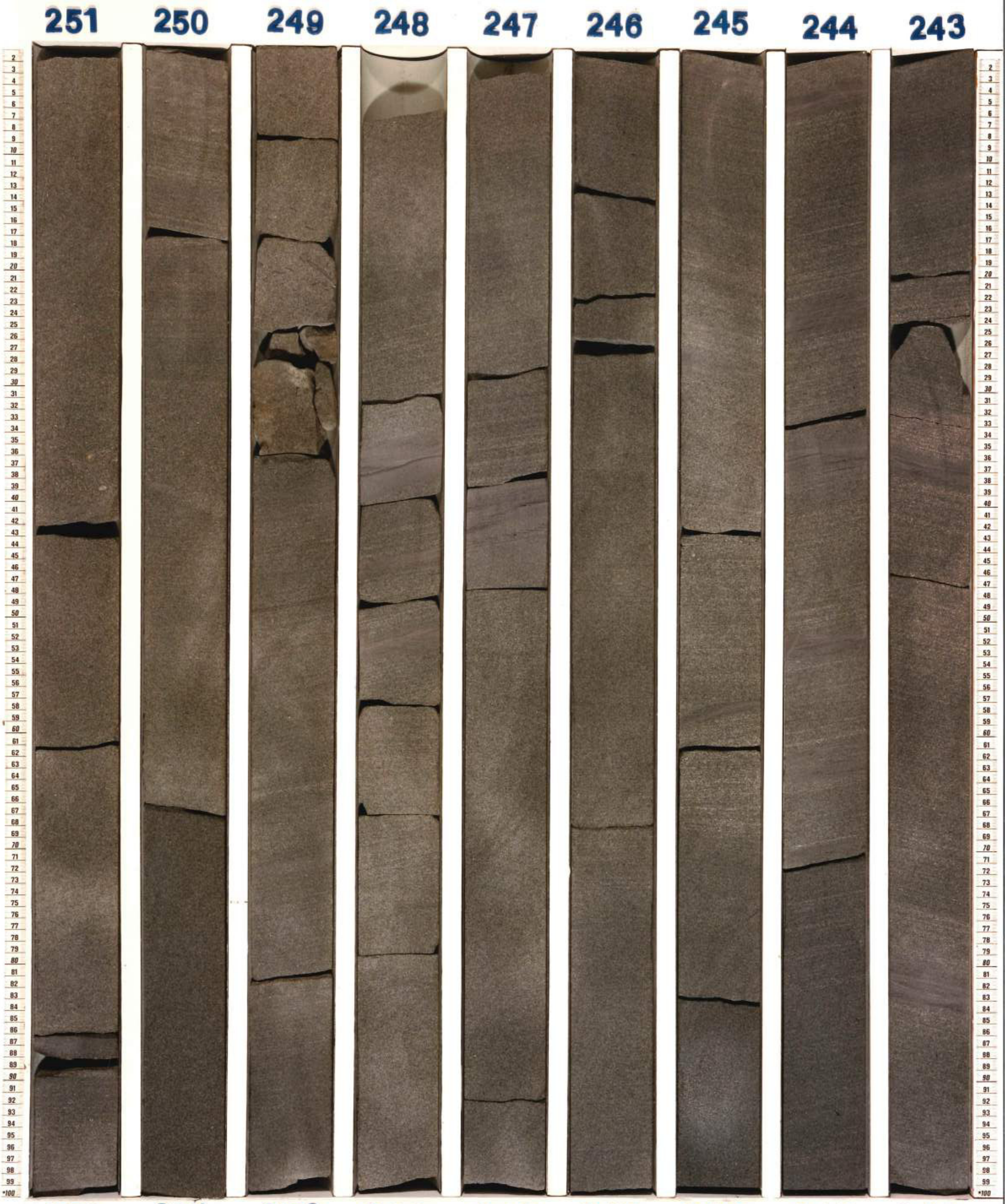

BOHRUNG GURTEN

UNIVERSITÄT BERN 1989

260 259 258 257 256 255 254 253 252

261 260 259 258 257 256 255 254 253

BOHRUNG GURTEN

UNIVERSITÄT BERN 1989